ISSN 0965-545X, Polymer Science, Ser. A, 2010, Vol. 52, No. 6, pp. 614–620. © Pleiades Publishing, Ltd., 2010.
Original Russian Text © E.G. Rukhlya, L.M. Yarysheva, A.L. Volynskii, N.F. Bakeev, 2010, published in Vysokomolekulyarnye Soedineniya, Ser. A, 2010, Vol. 52, No. 6, pp. 949–955.

The Effect of Strain Rate on Solvent Crazing of Poly(ethylene terephthalate) in Solutions of Poly(ethylene oxide) of Various Molecular Masses[1]

E. G. Rukhlya, L. M. Yarysheva, A. L. Volynskii, and N. F. Bakeev

Faculty of Chemistry, Moscow State University, Moscow, 119991 Russia
e-mail: katrin310@yandex.ru

Received September 21, 2009;
Revised Manuscript Received November 30, 2009

Abstract—The effect of strain rate on the behavior of PET during its tensile drawing in highly viscous liquids, such as liquid PEG (M 400) and semidilute solutions of PEO ($M = (4 \times 10^4)$–(1×10^6)), is studied. With an increase in strain rate, the mechanism of tensile drawing of PET in PEG changes from solvent crazing to shearing; at the same time, over the selected interval of strain rates, tensile drawing of PET in semidilute solutions of PEO proceeds via the mechanism of solvent crazing. During tensile drawing of PET in PEO solutions, the behavior of PET is almost the same as the mechanism of tensile drawing in a pure solvent. This result indicates that, in the course of flow of the polymer solution through the formed porous structure, PEO is filtered off in the local tip region of the growing craze.

DOI: 10.1134/S0965545X10060076

INTRODUCTION

Cold drawing of amorphous glassy polymers in adsorptionally active liquid media (AALMs) proceeds via the mechanism of classical solvent crazing, a process that is accompanied by the development of a specific mode of porosity [1–9]. AALMs are solvents in which a polymer undergoes almost no swelling but has a lowered surface tension. However, AALMs should satisfy another requirement related to the kinetics of the transport of a liquid into a tip of a growing craze. For the effective development of crazing, liquid should be quick enough to penetrate the tip of the growing craze. In the opposite case, tensile drawing of the polymer proceeds as that in air via necking. In [10–12], conditions providing for the development of crazing have been described; these conditions are controlled by the kinetics of craze growth and by the rate of liquid flow in the porous structure. One of the parameters controlling the flow rate of the liquid is its viscosity, and the transition from crazing to shear deformation is most pronounced during the tensile drawing of polymers in highly viscous liquids at high strain rates.

Most studies on solvent crazing of amorphous glassy and semicrystalline polymers have been performed for low-molecular-mass AALMs, and their viscosity does not exceed 40 cP (oleic acid) [9]. However, as was shown in earlier studies [13, 14], tensile drawing of polymers via the mechanism of solvent crazing can proceed not only in low-molecular-mass liquids but also in the presence of liquid oligomers. In particular, despite their high viscosity, such liquid oligomers as PEG and PPG are efficient AALMs with respect to PET and HDPE. In the above liquids, tensile drawing of polymers proceeds via the mechanism of solvent crazing, a process that is accompanied by the development of a nanoporous structure in the samples. Moreover, in PET and HDPE, this deformation mechanism can occur even in more viscous solvents, namely, in semidilute solutions of flexible-chain polymers with $M > 1 \times 10^6$ [15, 16].

The interest in the above studies is primarily due to the fact that this deformation is accompanied by the development of a nanoporous structure that is filled with the surrounding solution. When tensile drawing is performed in a solution containing various low-molecular-mass compounds, they penetrate into the as-formed porous structure; as a result, there is development of a composite in which both the polymer and the loaded compound are finely dispersed down to the nanoscale level. When tensile drawing of the polymer sample is done in the presence of liquid oligomers or in solutions of high-molecular-mass compounds, they too are able to penetrate the nanoporous structure of crazes. As a result, polymer–oligomer or polymer–polymer blends are formed. Since the viscosity of solutions markedly exceeds the viscosity of the earlier used

[1] This work was supported by the Russian Foundation for Basic Research, project no. 09-03-00430-a; by a Grant for the Support of Leading Scientific Schools, NSh-2467.2008.3; and by State Contract no. P1484.

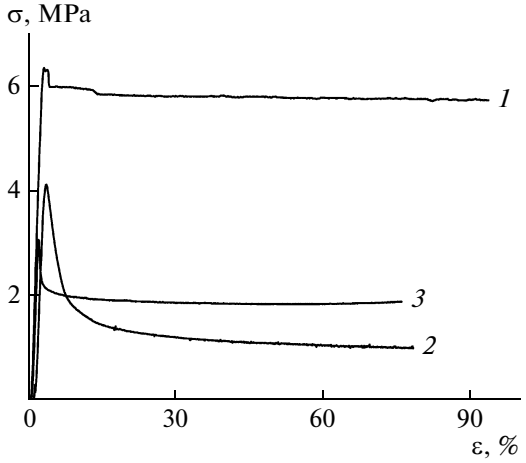

Fig. 1. Stress–strain curves illustrating tensile drawing of PET in (*1*) air, (*2*) PEG, and (*3*) isopropanol.

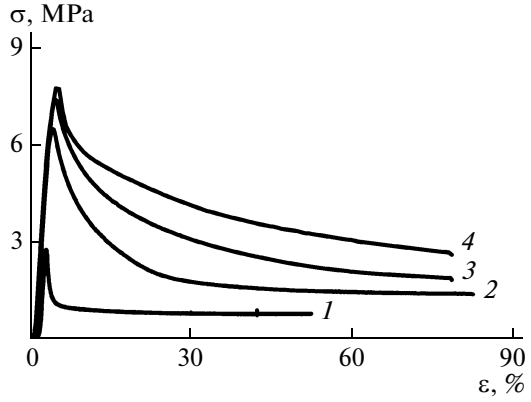

Fig. 2. Stress–strain curves illustrating tensile drawing of PET in PEG 400. The strain rates are (*1*) 0.2, (*2*) 5.4, (*3*) 10, and (*4*) 20 mm/min.

low-molecular-mass AALMs, it is necessary to verify whether these liquids can serve as efficient AALMs and to determine what effect the strain rate has on the mechanism of deformation.

The objective of this study is to investigate the effect of strain rate on the mechanical behavior of PET during tensile drawing in the presence of such highly viscous liquids as liquid oligomers (PEG) and solutions of PEO with $M = (4 \times 10^4)$–(1×10^6).

EXPERIMENTAL

In this study, we used films of amorphous unoriented PET with a thickness of 100 μm. Prior to tensile drawing, the films were mechanically pretreated in the presence of isopropanol in order to generate numerous surface defects and to provide nucleation of the maximum number of crazes. Test samples with a gage size of 6.15 × 20 mm were stretched on an Instron 4301 universal tensile machine at a constant strain rate of 0.2–260 mm/min in the presence of PEG with $M =$ 400 (PEG 400) as well as in a 20% water–ethanol solution of PEO with $M > 10 \times 10^5$ and in a 5% water–ethanol solution of PEO with $M = 1 \times 10^6$ (Aldrich). The porosity of the solvent-crazed sample was estimated as the ratio of volume gain ΔV achieved by tensile drawing and volume of the deformed polymer $V_0 + \Delta V$: $W = \Delta V/(V_0 + \Delta V)$, where V_0 is the initial volume of the polymer.

The geometric dimensions of the solvent-crazed PET sample stretched by a given tensile strain were measured with a projector with a tenfold magnification and an IZV-2 optimeter; the measurement error was ±1 μm. After tensile drawing in solutions of high-molecular-mass compounds, the crazed samples were dried in vacuum until attainment of a constant mass in order to remove the residual solvent and the content of PEO in the blend was estimated via weighing.

RESULTS AND DISCUSSION

In the case of tensile drawing of polymers in highly viscous liquids, there are certain limitations on the selection of stain rates. These limitations are associated with the transport constraints for the penetration of a liquid medium into the sites of local active deformation in a polymer sample (or into the tip of a growing craze) [10–12] and with changes in the mechanism of deformation. The most dramatic changes in the mechanism of deformation are observed in the course of investigating the mechanical response of a polymer to tensile drawing in the presence of a liquid medium. Figure 1 presents the stress–strain curves illustrating tensile drawing of PET in air (curve *1*) and in the presence of the liquid oligomer PEG 400 (curve *2*) at a strain rate of 0.2 mm/min. Figure 1 shows the stress–strain curve for the tensile drawing of PET in a typical low-molecular-mass AALM, such as isopropanol (curve *3*). As follows from Fig. 1, tensile drawing in the presence of a liquid medium (in isopropanol and liquid oligomer) is accompanied by a marked decrease in the tensile stress in PET relative to that in air, a behavior that is typical of polymers under tensile drawing via the mechanism of classical solvent crazing [1, 5, 9].

The mechanical behavior of polymers during tensile drawing in an AALM is directly associated with the character of craze evolution: craze nucleation, craze-tip advance, and craze thickening. As was mentioned in [5, 9], analysis of the stress–strain curves makes it possible to estimate the efficacy of the separate stages of craze evolution. Nucleation of crazes commences when the critical strain is attained; on the stress–strain curve, this process corresponds to the region below the yield point. The yield tooth is related to the stage of

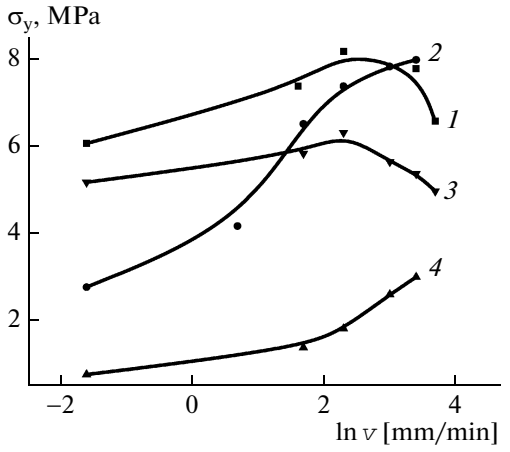

Fig. 3. (*1*, *2*) Yield stress and (*3*, *4*) postyield stress during tensile drawing of PET in (*1*, *3*) air and (*2*, *4*) PEG 400.

propagation of the fastest growing crazes (or their ensemble) through the whole cross section of the sample, while the postyield stress on the stress–strain curve is associated with the propagation of all nucleated crazes through the whole cross section of the sample (the stage of craze-tip advance); this stage is followed by the stage of craze thickening. Therefore, the profile of the stress–strain curve illustrating tensile drawing of a polymer in an AALM is controlled by the number of nucleated crazes and by the kinetics of their growth. In turn, the rates of craze-tip advance and craze thickening depend on the rate of liquid delivery to the porous structure and on the strain rate. This scenario of crazing evolution shows that the mechanism of deformation and, hence, the mechanical response of the polymer sample are controlled by the interplay between the strain rates and viscous flow of a liquid in the local deformation region.

During tensile drawing of polymer samples in liquid media, kinetic constraints related to the rate of liquid transport are mostly pronounced in the course of investigating the mechanical characteristics over a broad interval of strain rates. Earlier, these studies were performed for PVC and PET and for diverse low-molecular-mass AALMs [12–14]. For each liquid, there is a certain critical strain rate above which a liquid exerts no effect on yield stress. The higher the viscosity of the liquid, the lower the critical strain rate at which the mechanism of tensile drawing is changed.

Figure 2 presents the stress–strain curves illustrating tensile drawing of PET in PEG 400 over a broad interval of strain rates. At low strain rates, the stress–strain diagrams are traditional and include a linear initial region, a yield tooth, and a well-pronounced postyield plateau region. With an increase in the strain rate, the main changes occur in the postyield plateau region in the stress–strain curves. When tensile drawing of PET proceeds at a low strain rate, the yield tooth is followed by a marked stress decrease and the stress–strain curve approaches its plateau region. With an increase in strain rate, the stress drop after the yield point is not sharp and the transition to the stationary or postyield tensile stress is shifted toward higher tensile strains.

The above changes in the stress–strain curves are characteristic of the tensile drawing of PET in typical AALMs, a circumstance that is due to the phenomenon called the *effect of multiple sites of localized plastic deformation* [5, 7, 17]. As was shown in [18–21], when strain rate increases, the number of nucleated crazes increases and their growth-rate distribution becomes broader. As a result, the stress–strain curve approaches the plateau region at higher tensile strains.

Let us compare the strain-rate dependence of the mechanical characteristics for the tensile drawing of PET in PEG 400 and in air (Fig. 3).

During tensile drawing of PET in air, the yield stress and postyield stress linearly depend on the logarithm of strain rate, an observation that agrees well with the classical concepts of the deformation of glassy polymers and with the relevant Lazurkin and Eyring equations. Moreover, for tensile drawing of PET in air at high strain rates, yield stress and postyield stress decrease. This phenomenon has been discussed in the literature, and its cause is the hindrance of the removal of heat from the deformed sample [22]. When PET is stretched in the liquid medium, the conditions of heat removal are improved, a circumstance that makes it possible to explain the behavior of PET at higher strain rates.

As follows from Fig. 3, when PET is stretched in PEG 400 (curve *4*), yield stress at low strain rates is lower than that in air. However, as strain rate increases up to ~10 mm/min, yield stress approaches a level that is characteristic of tensile drawing in air.

For tensile drawing of PET in PEG 400, postyield stress increases with an increase in strain rate, as is the case in air. At strain rates above 10 mm/min, the increase in tensile stress is more pronounced during tensile drawing in the presence of a liquid medium. However, at all strain rates, postyield stress for the tensile drawing in liquid remains lower than that in air.

The observed changes in the mechanical characteristics of PET with variation in strain rate are indicative of the transition to the mixed mechanism of deformation at high strain rates, when crazing is aggravated by the onset of shearing deformation. In [10–12], several examples demonstrate the mixed mechanism of tensile drawing for PET in an AALM, when, at the initial stage of stretching, a neck is formed and, at later stages when stress drops after the yield point, crazes are nucleated and grow. The higher the viscosity of the liq-

uid, the lower the strain rate at which the transition to the mixed mechanism of deformation is observed. Evidently, the same character of deformation is observed for the tensile drawing of PET in PEG 400 at high strain rates, when, during tensile drawing in liquid, the yield stress practically corresponds to that in air and the postyield stress does not approach a level that is typical of tensile drawing in air.

Therefore, the mechanical behavior of PET in highly viscous PEG follows the same scenario as tensile drawing in typical low-molecular-mass AALMs In other words, liquid oligomers can be treated as typical AALMs, but their high viscosity exerts a marked effect on the strain-rate dependences of the mechanical characteristics. As was shown in [13, 14], the compositions of the resultant oligomer–polymer blends are controlled by the overall porosity of the solvent-crazed polymer, and the content of oligomer in PET can exceed 45%.

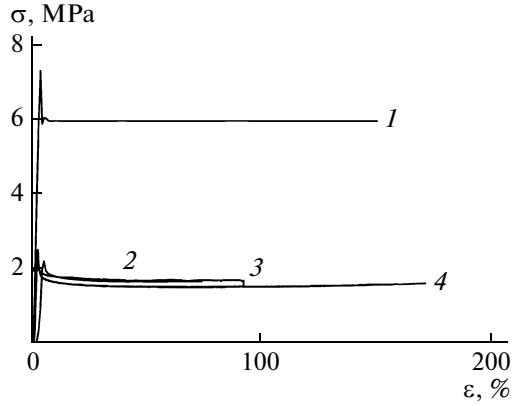

Fig. 4. Stress–strain curves illustrating tensile drawing of PET at a strain rate of 6 mm/min: in (*1*) air, (*2*) a water–ethanol solution, and (*3, 4*) water–ethanol solutions of PEO with molecular masses of $M = (3)\ 1 \times 10^6$ and (*4*) 4×10^4 and a concentration of 5.5%.

Let us discuss whether the above-mentioned features of crazing are preserved when PET samples are subjected to tensile drawing in the presence of polymers with higher molecular masses. To study the specific features of crazing of PET in the presence of high-molecular-mass compounds, PEO samples with a narrow molecular-mass distribution are selected, thereby making it possible to analyze the effect of the molecular mass of the added polymer on the crazing behavior of PET. At room temperature, PEOs are solid compounds; for experiments, their solutions in water–ethanol mixtures are used. In this case, water is used as a solvent for PEO, while ethanol is used as an AALM for PET. In the solution, the polymer concentration is 5.5–18.6%; i.e., this concentration exceeds the crossover, a circumstance that corresponds to the regime of semidilute solutions.

Figure 4 presents the stress–strain curves for the tensile drawing of PET in water–ethanol solutions of PEO with different molecular masses (curves *1*, *3*); the strain rate is constant (6 mm/min). For comparison, this figure shows the stress–strain curves for the tensile drawing of PET in air (curve *2*) and in a typical AALM, a PEO-free water—ethanol solution (curve *4*).

The stress–strain curves illustrating the tensile drawing of PET in the polymer solution, as well as the stress–strain curves for tensile drawing of PET in air and in typical AALMs, are characterized by well-pronounced yield tooth and postyield plateau regions. In comparison to tensile drawing in air, tensile drawing of PET in PEO solutions is accompanied by a marked decrease in tensile stress, a phenomenon that is a feature of solvent crazing in polymers [5, 9]. This outcome demonstrates that tensile stress in the polymer solution is comparable to that in the polymer-free water–ethanol solution. This circumstance indicates the high efficacy of solvent crazing in PEO solutions, although their viscosities are high.

Stress–strain curves illustrating the tensile drawing of PET at different strain rates were recorded in water–ethanol solutions of PEO with a concentration of 5.5%. The results are presented in Figs. 5a and 5b; Fig. 5c corresponds to the tensile drawing of PET in a 20% solution of PEO with $M = 4 \times 10^4$. For comparison, Fig. 5d presents the stress–strain curves for the tensile drawing of PET in the PEO-free water–ethanol solution.

Although the viscosities of all solutions are high, the stress–strain curves of PET slightly depend on the molecular mass and concentration of PEO; these curves are almost the same as the stress–strain curves of PET in a pure-water–ethanol solution. In all cases, the stress–strain curves show a well-pronounced yield tooth and postyield region. The higher the strain rate, the higher the tensile strain at which the stress–strain curve of the polymer approaches the plateau region.

Figure 6 presents the yield stress plotted against strain rate for the tensile drawing of PET in PEO solutions with different molecular masses (curves *3–5*) and in the same PEO-free water–ethanol solution (curve *2*). For comparison, this figure shows the yield stress plotted against strain rate for tensile drawing of PET in air (curve *1*). As follows from Fig. 6, over the entire interval of variations in the strain rate, the yield stress is lower for PET in the PEO solution than for PET in air, an observation that is typical of the deformation via solvent crazing. In the polymer solution, the strain-rate dependences of yield stress practically coincide with those for the tensile drawing of PET in the PEO-free water–ethanol solution (curve *2*). This result indicates that, in the presence of polymer in the

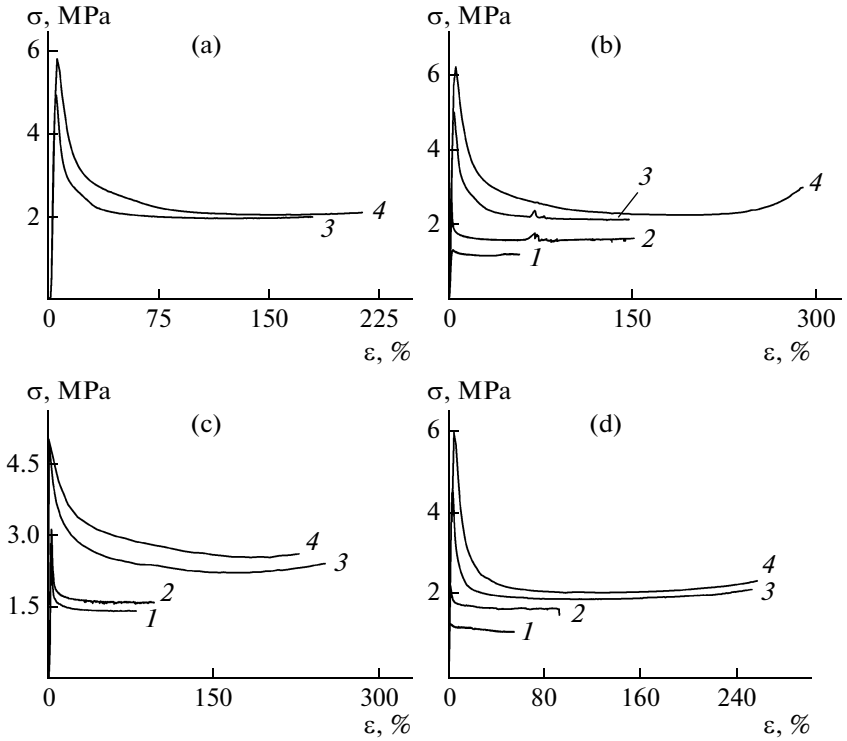

Fig. 5. Stress–strain curves illustrating tensile drawing of PET in (a–c) PEO solutions with concentrations of (a, b) 5.5% and (c) 20.0% and (d) a water–ethanol solution. The strain rates are (*1*) 0.2, (*2*) 6, (*3*) 100, and (*4*) 265 mm/min. The molecular masses of PEO are (a, c) 4×10^4 and (b) 1×10^6.

solution, the efficacy of crazing does not decrease over the entire interval of strain rates.

In addition, the conclusion that, over the entire interval of selected strain rates, tensile drawing of PET in PEO solutions proceeds via the mechanism of solvent crazing can be verified by the data on porosity. The porosity of PET samples after tensile drawing in the solutions of PEO with different molecular masses remains high, and, within the selected interval of strain rates, this parameter is independent of strain rate, as in the case of tensile drawing in the water–ethanol solutions.

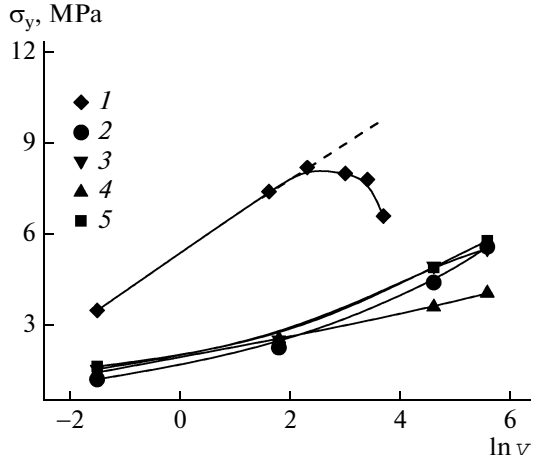

Fig. 6. Yield stress plotted against strain rate for the tensile drawing of PET: in (*1*) air; (*2*) a water–ethanol solution; and (*3–5*) PEO solutions with $M =$ (*3*) 4×10^4, (*4*) 4×10^5, and (*5*) 1×10^6; the concentration of PEO solutions is 5.5%.

Analysis of the stress–strain curves for the tensile drawing of PET in PEO solutions makes it possible to estimate the rate of craze growth and, consequently, the flow rate of the polymer solution. In [15, 16], the correlation between the mechanical behavior of the polymer during tensile drawing in AALMs via the mechanism of solvent crazing and various stages of craze evolution has been established. In particular, it was shown that the postyield region corresponds to craze propagation through the whole cross-sectional area of the sample. In this context, with knowledge of the stretching time and geometric dimensions of the sample, it is possible to estimate the effective linear craze growth rate. As was shown in [23], craze growth rates calculated from stress–strain curves are comparable to the craze growth rates estimated from the direct measurements of the craze-tip advance rate for individual crazes during tensile drawing of PET in an AALM. Analysis of the stress–strain curves illustrating the tensile drawing of PET in PEO solutions in the

Variations in craze growth rate v_c during tensile drawing of PET in water–ethanol solutions of PEO of various molecular masses at different strain rates

Medium	Molecular mass	c, %	v_c, mm/min, at some strain rate (mm/min)			
			0.2	6	100	265
Ethanol–water solution	–	–	0.3	2.3	26.0	60.0
PEO	4×10^4	20.0	0.1	1.3	10.0	22.0
	4×10^4	5.5	–	–	18.7	38.5
	1×10^5	5.5	–	2.1	22.7	44.5
	4×10^5	5.5	0.2	1.5	20.0	40.0
	1×10^6	5.5	0.1	2.0	23.0	34.2

region corresponding to the transition to the stationary regime of deformation makes it possible to estimate the effective craze growth rate as a function of the strain rate and molecular mass of PEO in the solution. This evidence is summarized in the table. In the case of tensile drawing of PET in semidilute polymer solutions, the effective linear craze growth rate is comparable with the craze growth rate in a pure solvent, although their viscosities are appreciably different. It is possible to observe in the craze growth rate only a slight decrease, which becomes more pronounced with an increase in the concentration and molecular mass of the polymer.

Therefore, tensile drawing of PET in the solutions of high-molecular-mass PEO proceeds via the mechanism of solvent crazing, a process that is accompanied by the development of a porous structure. Analysis of the mechanical behavior of PET in the solutions of high-molecular-mass PEO makes it possible to conclude that craze evolution is primarily controlled by the solvent, which serves as an AALM. Its penetration into the craze tip controls the rate of craze growth and the behavior of PET during its tensile drawing in an AALM. However, as was shown in [15, 16], high-molecular-mass PEO macromolecules from semidilute solutions are likewise able to penetrate to the as-formed porous structure. This process can be explained as follows: The polymer solution is drawn into the porous structure owing to the negative hydrodynamic pressure at the boundary of the formed craze. In this case, PEO molecules in the solution are delivered into the porous structure of crazes by a flowing solvent, but they are not delivered into the tip of the growing craze and, thus, do not affect the efficacy of solvent crazing.

Therefore, when the strain rate increases, tensile drawing of PET in the liquid oligomer (PEG 400) is associated with the change in the mechanism of deformation from solvent crazing to shearing. Over the entire interval of strain rates under study, tensile drawing of PET in the solutions of high-molecular-mass PEO proceeds via the mechanism of solvent crazing in a way similar to that of tensile drawing in a pure solvent, which is an AALM. This fact suggests that, in the local region of a growing craze tip, the polymer is filtered off. This filtering happens in the course of the flow of the polymer solution through the porous structure of a craze, while the craze tip is filled with a solvent whose viscosity is close to the viscosity of a pure solvent. Analysis of the stress–strain curves makes it possible to estimate the effective craze growth rate and, hence, the rate of flow of the polymer solution into the local region of a growing craze.

REFERENCES

1. R. P. Kambour, J. Macromol. Sci., Rev. Macromol. Chem. **7**, 1 (1973).
2. E. J. Kramer, Adv. Polym. Sci. **52–53**, 2 (1983).
3. E. J. Kramer and L. Berger, Adv. Polym. Sci. **91–92**, 1 (1990).
4. L. M. Yarysheva, G. M. Lukovkin, A. L. Volynskii, and N. F. Bakeev, *Features of Rehbinder Effect in Polymers* (Nauka, Moscow, 1992) [in Russian].
5. A. L. Volynskii and N. F. Bakeev, *Solvent Crazing of Polymers* (Elsevier, Amsterdam, 1995).
6. A. L. Volynskii, Priroda (Moscow, Russ. Fed.), No. 11, 11 (2006).
7. A. L. Volynskii and N. F. Bakeev, *Structural Self-Organization of Amorphous Polymers* (Fizmatlit, Moscow, 2005) [in Russian].
8. R. Estevez, M. G. A. Tijssens, and E. Van der Giessen, J. Mech. Phys. Solids **48**, 2585 (2000).
9. A. L. Volynskii and N. F. Bakeev, *Highly Dispersed Oriented State of Polymers* (Khimiya, Moscow, 1985) [in Russian].
10. A. L. Volynskii, N. A. Shitov, and N. F. Bakeev, Vysokomol. Soedin., Ser. A **23**, 859 (1981).
11. A. L. Volynskii, N. A. Shitov, and N. F. Bakeev, Vysokomol. Soedin., Ser. A **23**, 978 (1981).
12. N. A. Shitov, Candidate's Dissertation in Chemistry (Moscow, 1983).
13. E. G. Rukhlya, O. V. Arzhakova, L. M. Yarysheva, et al., Polymer Science, Ser. B **49** (2007) [Vysokomol. Soedin., Ser. B **49**, 920 (2007)].

14. E. G. Rukhlya, O. V. Arzhakova, A. A. Dolgova, et al., Int. J. Polym. Anal. Charact. **12**, 65 (2007).
15. E. G. Rukhlya, L. M. Yarysheva, A. L. Volynskii, and N. F. Bakeev, Polymer Science, Ser. B **49** (2007) [Vysokomol. Soedin., Ser. B **49** 1876 (2007)].
16. A. L. Volynskii, E. G. Rukhlya, L. M. Yarysheva, and N. F. Bakeev, Ross. Nanotekhnol. **2** (5-6), 44 (2007).
17. G. M. Lukovkin, Doctoral Dissertation in Chemistry (Moscow, 1986).
18. A. L. Volynskii, L. M. Yarysheva, and N. F. Bakeev, Polymer Science, Ser. C **43** (2001) [Vysokomol. Soedin., Ser. C **43**, 2289 (2001)].
19. L. M. Yarysheva, I. V. Chernov, L. Yu. Kabal'nova, et al., Vysokomol. Soedin., Ser. A **31**, 1544 (1989).
20. L. M. Yarysheva, L. Yu. Pazukhina, T. A. Borodulina, et al., Vysokomol. Soedin., Ser. A **26**, 2380 (1984).
21. L. M. Yarysheva, L. Yu. Pazukhina, N. M. Kabanov, et al., Vysokomol. Soedin., Ser. A **26**, 388 (1984).
22. A. S. Kechek'yan, G. P. Andrianova, and V. A. Kargin, Vysokomol. Soedin., Ser. A **12**, 2424 (1970).
23. L. M. Yarysheva, A. A. Dolgova, O. V. Arzhakova, et al., Polymer Science, Ser. A **44** (2002) [Vysokomol. Soedin., Ser. A **44**, 1359 (2002)].